Segregation of leading-edge and uropod components into specific lipid rafts during T cell polarization

Concepción Gómez-Moutón*, Jose Luis Abad*, Emilia Mira*, Rosa Ana Lacalle*, Eduard Gallardo†, Sonia Jiménez-Baranda*, Isabel Illa†, Antonio Bernad*, Santos Mañes*‡, and Carlos Martínez-A.*

*Department of Immunology and Oncology, Centro Nacional de Biotecnología, Consejo Superior de Investigaciones Científicas, Universidad Autónoma de Madrid, Cantoblanco, E-28049 Madrid, Spain; and †Laboratorio de Neurología Experimental, Santa Creu i Sant Pau Hospital, 08025 Barcelona, Spain

Edited by Kai Simons, Max Planck Institute of Molecular Cell Biology and Genetics, Dresden, Germany, and approved June 11, 2001 (received for review April 2, 2001)

Redistribution of specialized molecules in migrating cells develops asymmetry between two opposite cell poles, the leading edge and the uropod. We show that acquisition of a motile phenotype in T lymphocytes results in the asymmetric redistribution of ganglioside GM3- and GM1-enriched raft domains to the leading edge and to the uropod, respectively. This segregation to each cell pole parallels the specific redistribution of membrane proteins associated to each raft subfraction. Our data suggest that raft partitioning is a major determinant for protein redistribution in polarized T cells, as ectopic expression of raft-associated proteins results in their asymmetric redistribution, whereas non-raft-partitioned mutants of these proteins are distributed homogeneously in the polarized cell membrane. Both acquisition of a migratory phenotype and SDF-1α-induced chemotaxis are cholesterol depletion-sensitive. Finally, GM3 and GM1 raft redistribution requires an intact actin cytoskeleton, but is insensitive to microtubule disruption. We propose that membrane protein segregation not only between raft and nonraft domains but also between distinct raft subdomains may be an organizational principle that mediates redistribution of specialized molecules needed for T cell migration.

Cell movement across a two-dimensional substrate requires a dynamic interplay between attachment at the cell front and detachment at the rear cell edge, combined with a traction machinery that pulls the net cell body forward. As adhesion and detachment occur at opposite cell edges, the moving cell must acquire and maintain spatial and functional asymmetry, a process called polarization (1, 2). This asymmetry develops between two opposite cell edges—the leading edge, which protrudes, and the rear (termed uropod in lymphocytes), which retracts.

Because of the specialized functions of these compartments, each pole in migrating cells is enriched in specific receptors and signaling molecules but lacks others. In fibroblast-like cells and lymphocytes, the leading edge contains chemokine receptors, several glycosylphosphatidylinositol-linked proteins, such as the urokinase plasminogen activator receptor (uPAR), as well as the machinery that senses the environment and induces localized actin polymerization (1). Whereas the rear edge in fibroblasts appears to be a passive tail, the lymphocyte uropod is a specialized pseudopod-like projection with important functions, including motility and recruitment of bystander cells. Several intercellular adhesion molecules (ICAMs) concentrate at the uropod, including ICAM-1, -2 and -3, CD43, CD44, as well as the actin-binding proteins of the ezrin–radixin–moesin family. In accordance with its importance in lymphocyte migration, crosslinking of molecules located in the uropod is sufficient to trigger neutrophil polarization and motility (3).

To understand polarization and chemotaxis processes, the molecular mechanisms involved in the generation and maintenance of the asymmetric distribution of cell-surface components must be elucidated. Several lines of evidence suggest that association of proteins with cholesterol- and glycosphingolipid-enriched raft-membrane domains is crucial in distributing specialized molecules to the leading edge of fibroblast-like migrating cells. The raft marker GM1 ganglioside, the raft-associated chemokine receptor CCR5, and other raft-associated proteins accumulate preferentially at the leading lamella of migrating cells (4). Modification of raft-located proteins such that they no longer associate with rafts inhibits their asymmetric redistribution. The functional role of asymmetric raft redistribution is shown in this article, as membrane cholesterol depletion impairs cell polarization and chemotaxis. Cholesterol-depleted cells showed isotropic pseudopodial protrusion, suggesting that raft redistribution is needed for location-specific induction of pseudopod protrusion during cell polarization. Moreover, rafts are the preferred cell platforms for membrane-linked actin polymerization by *in situ* phosphatidylinositol 4,5-bisphosphate synthesis and tyrosine kinase signaling through the WASP-Arp2/3 pathway (5–7).

Raft association seems to be pivotal for protein redistribution to the leading edge in migrating cells. To analyze whether this process is a general mechanism in all cell types, we studied redistribution of raft-associated membrane receptors and lipids during T cell polarization, and found that membrane rafts are redistributed asymmetrically in migrating T lymphocytes. In contrast to the exclusive leading-edge redistribution detected in fibroblast-like cells, polarized T lymphocytes segregate leading-edge and uropod markers into two raft types that differ in lipid and protein composition. Leading-edge rafts, characterized by including chemokine receptors and uPAR, are enriched in GM3 ganglioside and devoid of GM1; uropod rafts, containing CD44 and other cell-adhesion molecules, are enriched in GM1 but lack GM3.

Ectopic expression of the raft-associated influenza virus hemagglutinin (HA) results in its asymmetric distribution in polarized T cells, whereas expression of a nonraft mutant version (HA2A520; ref. 8) results in homogeneous protein distribution on the cell membrane. We observed asymmetrical redistribution of a green fluorescent protein (GFP)-tagged version of the vesicular stomatitis virus glycoprotein (VSVG3)-GFP (9) that colocalizes with GM1 when expressed in T cells. A mutant version of this protein (VSVG3-SP-GFP; ref. 10), which does not colocalize with GM1, is distributed homogeneously on the cell membrane. These data suggest that raft partitioning is a major determinant of asymmetric protein redistribution in polarized T cells. Accordingly, membrane cholesterol depletion impedes acquisition of a polarized cell phenotype and inhibits both cell–cell interaction and cell chemotaxis. All together, the results indicate a prominent role for membrane rafts in the acquisition of the polarity needed for T cell chemotaxis.

This paper was submitted directly (Track II) to the PNAS office.

Abbreviations: uPAR, urokinase plasminogen activator receptor; ICAM, intercellular adhesion molecule; HA, hemagglutinin; GFP, green fluorescent protein; VSVG3, vesicular stomatitis virus glycoprotein 3; CTx, cholera toxin β-subunit; CD, methyl-β-cyclodextrin; PBLs, peripheral blood lymphocytes; DRM, detergent-resistant membranes.

See commentary on page 9471.

‡To whom reprint requests should be sent. E-mail: smanes@cnb.uam.es.

The publication costs of this article were defrayed in part by page charge payment. This article must therefore be hereby marked "*advertisement*" in accordance with 18 U.S.C. §1734 solely to indicate this fact.

www.pnas.org/cgi/doi/10.1073/pnas.171160298

Materials and Methods

Cell Culture, Expression Constructs, and Antibodies. The murine NS-1 T cell hybridoma and the human Jurkat cell line were cultured in RPMI medium 1640 with 5% (vol/vol) FCS, antibiotics, L-glutamine, and sodium pyruvate. The influenza virus HA wild type and the HA2A520 mutant, with two point mutations in the transmembrane domain that reduce raft association (8), were a gift of P. Scheiffele (Univ. of California, Berkeley). VSVG3-GFP and VSVG3-SP-GFP (9, 10), which is identical to VSVG3-GFP but has a spacer between the viral protein and the GFP moiety, were given by P. Keller (Max Planck Institute, Molecular Cell Biology and Genetics, Dresden, Germany). All constructs were subcloned into the pLZR retroviral vector; NS-1 cells were transduced with the recombinant retrovirus (11).

Surfact-Amps X-100 with 10% (vol/vol) Triton X-100 and Surfact-Amps 58 with 10% (vol/vol) Brij58 were obtained from Pierce. Optiprep gradient medium was obtained from Nycomed Pharma, latrunculin-B from Calbiochem, and methyl-β-cyclodextrin (CD), demecolcine, water-soluble cholesterol, filipin III, fibronectin, BSA, peroxidase (PO)-conjugated streptavidin, biotin- and FITC-labeled cholera toxin β-subunit (CTx), and anti-talin monoclonal antibody (mAb) were obtained from Sigma. Anti-CXCR4 (Fab172B) and anti-human CD44 mAb were obtained from R & D Systems, rat anti-mouse CD44 and biotin-labeled anti-human CD43 from PharMingen, anti-mouse CD43 from Santa Cruz Biotechnology, and anti-transferrin receptor from Zymed. Rabbit anti-HA was a gift of P. Scheiffele, and PO- or Cy3-labeled secondary antibodies were obtained from Dako or Jackson ImmunoResearch.

Characterization of Anti-GM3 Antiserum. A serum sample from a patient with acute polyneuropathy was analyzed for IgM and IgG antibodies to GM1, GM2, GM3, aGM1, GD1a, GD1b, GD3, GT1b, and GQ1b by direct ELISA and TLC. ELISA titers were calculated by end-point dilution analysis of optical densities. For TLC, 1 μg per lane of each lipid was loaded onto a silica gel plate and developed by using a methanol, chloroform, and $CaCl_2$ solvent. After blocking with PBS/BSA, each plate was covered with 2.5 ml of diluted test serum (1/100) and incubated for 4 hr at 4°C. After washing, plates were incubated for 1 hr at 20°C with PO-conjugated IgM or IgG, as required. Serum reactivity to crude cell extracts (20 μg per lane) was analyzed by Western blotting.

Flotation Experiments. To analyze detergent-insoluble complexes in flotation gradients, 15×10^6 Jurkat cells stimulated with SDF-1α (100 nM, 15 min, 37°C; PeproTech, Rocky Hill, NJ) were cooled on ice, washed with PBS, and lysed in 300 μl of TNE buffer (50 mM Tris·HCl, pH 7.4/150 mM NaCl/5 mM EDTA) with 0.5% Triton X-100 or 1% Brij58. Cells were extracted for 20 min on ice and the extract was subsequently brought to 35% (vol/vol) Optiprep. One-third of the lysate was sequentially overlayered with 3.5 ml of 30% (vol/vol) Optiprep and 200 μl of TNE with detergent in an SW60 tube. After centrifugation (4 hr at 170,000 $\times$ *g* at 4°C), five fractions were collected from the gradient (top to bottom) and precipitated with trichloroacetic acid. Normalized protein amounts for each fraction were analyzed by SDS/PAGE and Western blotting.

For cholesterol depletion, serum-starved Jurkat cells were incubated with 5 mM CD for 30 min at 37°C. Under these conditions, CD treatment does not induce cell detachment from the substrate or modify viability (data not shown). After incubation, CD was removed by repeated washing with serum-free medium containing 0.01% BSA, then cells were stained with filipin as described (4). Flotation gradients of untreated and CD-treated cells were prepared as above.

Immunofluorescence and Antibody-Induced Patching. Resting peripheral blood lymphocytes (PBLs) were isolated from fresh human blood by Ficoll–Hypaque density-gradient centrifugation (Amersham Pharmacia), then plated in two adherence incubation steps at 37°C for 1 hr each in plastic flasks, then plated on recombinant human ICAM-2/Fc chimera protein (R & D Systems). NS-1 and Jurkat cells were plated on fibronectin (Fn)-coated eight-well-chamber glass slides 24 hr before assay. Serum-starved Jurkat cells and PBLs were stimulated with 100 nM SDF-1α, then washed and fixed with 3.7% (wt/vol) paraformaldehyde for 5 min on ice in PBS. Samples were incubated with the indicated antibodies, then with Cy2- or Cy3-conjugated second antibodies for 45 min on ice. For talin-staining, methanol-permeabilized cells (10 min, −20°C) were blocked with PBS/2% (wt/vol) BSA for 1 hr at 4°C before staining with primary antibodies. Slides were mounted in Vectashield medium containing 4′,6-diamidino-2-phenylindole (Vector Laboratories). In some experiments, NS-1 cells plated on Fn were treated at 37°C for 30 min with 10 μM latrunculin-B or 0.3 μM demecolcine, washed twice with medium, and fixed and stained with FITC-CTx and anti-CD44 or anti-GM3.

For HA and HA2A520 visualization in transduced NS-1 cells, antibody-mediated lateral copatching was performed by incubating unfixed cells for 30 min at 12°C with anti-HA and anti-GM3 antibodies. Further crosslinking was performed with Cy2- and Cy3-second antibody for 30 min at 12°C; antibody–receptor complex internalization was not seen. Cells were fixed and mounted as above. For HA copatching with CTx, FITC-CTx (6 μg/ml) was added after fixation and incubated for 10 min at 4°C; cells were methanol-fixed for 10 min at −20°C before mounting.

In all cases, cells were visualized by confocal laser scanning microscopy. Linear signal intensity for each fluorophore was covered by a linear scale of pixel intensities. The two colors were acquired separately and merged by using TCS NT software (Leica). Digital images were processed with PHOTOSHOP (Adobe).

Polarization, Cell–Cell Interaction, and Chemotaxis of Cholesterol-Depleted Cells. NS-1 cells were untreated or CD-treated as for Jurkat cells. A portion of the CD-treated cells was incubated for 30 min at 37°C in RPMI 1640 medium with 60 μg/ml free cholesterol. Untreated, CD-treated, or cholesterol-replenished cells were fixed with 3.7% (wt/vol) paraformaldehyde, then incubated with anti-CD44. Polarization was analyzed by confocal and phase-contrast microscopy.

For cell–cell interaction, Jurkat cells were untreated, treated with CD, or treated with CD plus cholesterol, then plated on fibronectin-coated chambers in the presence of SDF-1α (25 nM). After the addition of PBLs (7.5×10^4 cells per well), images were acquired in phase-contrast microscopy. Jurkat cells attached and spread on the substrate (phase-dark cells), and PBLs that adhered to the Jurkat cell uropod (phase-bright cells) were counted for each condition. Recruitment index is expressed as PBLs captured divided by the number of substrate-adhered Jurkat cells in the first layer.

For chemotaxis, Jurkat cells were untreated or treated with CD or CD plus cholesterol, resuspended, and migration-analyzed in a modified Boyden chamber (Costar). In all cases, 2×10^5 cells in serum-free medium were seeded in the upper chamber and the lower chambers were filled with serum-free medium alone or serum-free medium containing SDF-1α (25 nM). After incubation for 2.5 hr at 37°C, the cell number in the lower chamber was estimated by flow cytometry with an electronically programmable individual cell sorter. The chemotactic index was calculated as the quotient of the number of cells recovered in SDF-1α transwells and the number of cells in the absence of stimulus.

Results

GM1-Based Rafts Are Asymmetrically Distributed to the Migrating T Cell Uropod. We analyzed whether lipid rafts are asymmetrically redistributed in polarized T cells, as reported for fibroblast-like

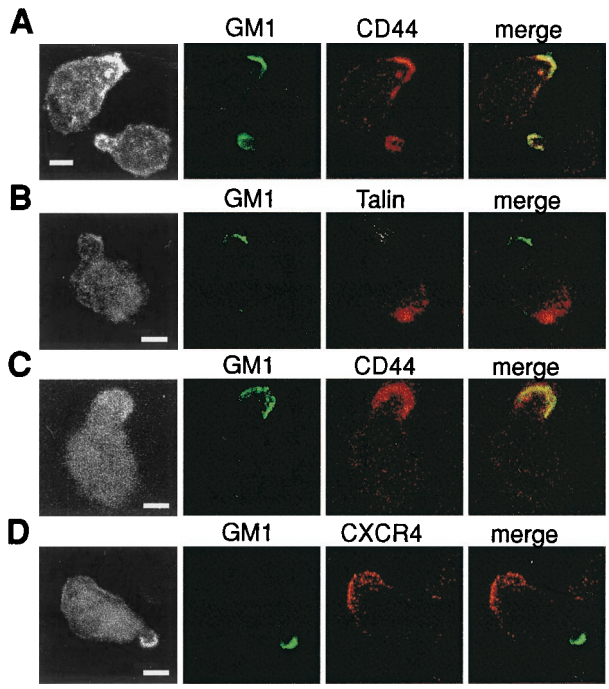

Fig. 1. GM1-rafts concentrate at the uropod of migrating T cells. NS-1 (*A* and *B*) or SDF-1α-stimulated Jurkat cells (*C* and *D*) were costained with CTx to reveal GM1 (green), with leading edge or uropod markers indicated (red), and analyzed by confocal microscopy. Fluorescence is shown for each signal and for the merging of both; colocalization is seen as yellow. To visualize cell shape (*Left*), laser power was saturated for green and red channels. These cells are representative of the majority of cells recorded in independent experiments. (Bar = 2 μm.)

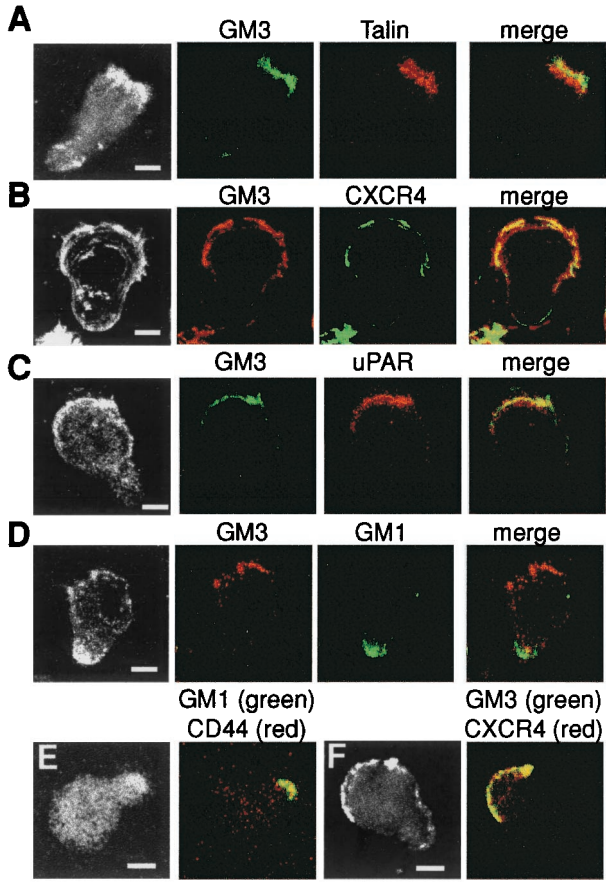

Fig. 2. GM1- and GM3-rafts segregate to opposite cell edges in T cells. Confocal analysis of NS-1 (*A* and *D*), SDF-1α-stimulated Jurkat cells (*B* and *C*), and SDF-1α-stimulated PBLs (*E* and *F*) costained with anti-GM3 antiserum or CTx and with various leading-edge and uropod markers, as indicated. For NS-1 and Jurkat cells, fluorescence for each channel and the merging of both signals are shown, whereas only merging is displayed for PBLs; colocalization of the signals is seen as yellow. (Bar = 2 μm.)

cells, by studying raft-enriched ganglioside GM1 distribution in constitutively polarized NS-1 cells. When plated on fibronectin, most NS-1 cells become polarized with a well defined leading edge and uropod. Compared with the homogeneous distribution in nonpolarized cells (data not shown), GM1 concentrated mainly at the NS-1 cell uropod, as determined by morphological criteria and by colocalization studies with uropod-specific markers such as CD44 (Fig. 1*A*). GM1 also appears at the edge opposite that at which leading-edge markers such as talin (12) are seen, confirming GM1 concentration at the NS-1 cell uropod (Fig. 1*B*).

It was unclear whether uropod GM1 concentration is unique to NS-1 cells or is a generalized phenomenon in polarized T cells. Therefore, we analyzed GM1 distribution in Jurkat cells stimulated with SDF-1α, a chemokine that induces CXCR4 redistribution to the leading edge of migrating Jurkat cells (13). GM1 patches redistribute to and colocalize with the uropod marker CD44 (Fig. 1*C*) but segregate to the pole opposite the CXCR4 staining (Fig. 1*D*). Collectively, these results indicate that GM1-based rafts and their associated proteins are distributed to the uropod in T cells with a migrating phenotype.

Leading-Edge Proteins in Migrating T Cells Colocalize with GM3-Rafts. Chemokine receptors such as CXCR4 partition into the raft fraction (14, 15), although CXCR4 does not colocalize with GM1 in T cells (Fig. 1*D*). Some glycosylphosphatidylinositol-anchored leukocyte-surface glycoproteins that accumulate at the leading edge associate preferentially to GM3 (16), suggesting that GM3-based rafts concentrate at the leading-cell edge. We analyzed GM3 distribution in migrating cells by using an antiserum from a patient with acute polyneuropathy with a high anti-GM3 titer (1/740) but no reactivity to a battery of other gangliosides including GM1. In addition, this antiserum does not react with cell proteins as analyzed by Western blotting (data not shown).

GM3 is asymmetrically distributed, forming patches at the same pole as talin (Fig. 2*A*) and colocalizing with other leading-edge markers such as CXCR4 (Fig. 2*B*) and uPAR (Fig. 2*C*). GM3 concentrates mainly at the edge opposite that of GM1 (Fig. 2*D*), which decorates the uropod (see above). These results indicate the existence of two distinct raft types in T cells, which segregate to opposite sides once the cell acquires a migrating phenotype; GM3-enriched rafts redistribute to the leading edge, and GM1-enriched rafts concentrate at the uropod. Segregation between leading rafts (L-rafts) and uropod rafts (U-rafts) is also seen in freshly isolated SDF-1α-stimulated PBLs; GM1 colocalizes with the uropod marker CD44 (Fig. 2*E*), and GM3 colocalizes with the leading-edge marker CXCR4 (Fig. 2*F*).

GM1- and GM3-Raft-Associated Proteins Partition in Detergent-Resistant Membranes. Raft-associated membrane proteins float in density gradients as detergent-resistant membranes (DRM; ref. 17); this property distinguishes them from insoluble complexes formed by cytoskeletal association. To analyze DRM partitioning of GM1- and GM3-associated proteins, we fractionated Jurkat cells lysed with the nonionic detergents Triton X-100 and Brij58. The leading-edge markers CXCR4, uPAR, and GM3, as well as the uropod markers CD44 and GM1, partition to the DRM fraction independently of the detergent used (Fig. 3*A*). Triton X-100 and Brij58

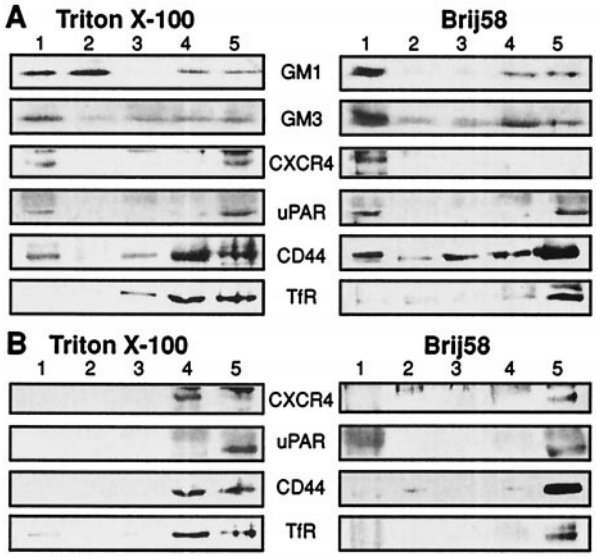

Fig. 3. GM1- and GM3-associated molecules partition in cholesterol-sensitive DRM. Jurkat cells were stimulated with SDF-1α, then left untreated (*A*) or CD-treated (*B*). Cells were lysed in TNE buffer with Triton X-100 or Brij58 and fractionated in Optiprep gradients. Fractions were collected from gradient top (DRM) to bottom (detergent-soluble proteins and cytoskeleton) and analyzed by Western blotting with the indicated antibodies; GM1 was detected with biotinylated CTx. TfR, transferrin receptor.

differ in their hydrophilic-lipophilic balance, a characteristic used to distinguish raft types in Madin–Darby canine kidney (MDCK) cells (18). Although Brij58 increases DRM-associated proteins and lipids, no differential solubility was detected between GM3- and GM1-associated markers in using the two detergents. Full solubilization of nonraft proteins such as the transferrin receptor confirms the quality of the fractionations.

CD treatment of Jurkat cells to sequester membrane cholesterol before fractionation resulted in increased CXCR4, uPAR, and CD44 solubility with either detergent (Fig. 3*B*). This result suggests that leading-edge and uropod-marker association to L- or U-rafts is sensitive to cholesterol extraction, although differences in cholesterol content for each raft type cannot be excluded.

Raft Association Is Needed for Membrane Protein Redistribution. We examined whether protein redistribution to the leading edge of the uropod is a consequence of specific association to GM3- or GM1-enriched rafts. NS-1 cells were transduced with retrovirus coding for the raft-associated influenza virus HA protein and the nonraft HA2A520 mutant (8). These cells were also transduced with two GFP-tagged versions of VSVG (VSVG3-GFP and VSVG3-SP-GFP). VSVG colocalizes with GM1 in several cell types, although it does not partition in DRM (19). Accordingly, neither VSVG3-GFP nor VSVG3-SP-GFP partition in DRM, but only VSVG3-GFP colocalizes with GM1 (see Fig. 4 *A* and *E*). The differential behavior of VSVG3-GFP and VSVG3-SP-GFP is not yet understood, although the masking of sorting signals in VSVG3-GFP may be implicated (9).

HA and VSVG3-GFP redistribute to the uropod in polarized NS-1 cells and colocalize with GM1 (Fig. 4 *A* and *C*) but segregate from GM3 rafts (Fig. 4 *B* and *D*). HA and VSVG3-GFP proteins probably do not associate to cytoskeleton or to other cell receptors; thus, their preferential accumulation in the uropod is solely the consequence of their U-raft association. Therefore, we expressed the nonraft HA mutant (HA2A520) and the basolateral-sorted VSVG3-SP-GFP and analyzed their distribution in polarized NS-1. HA2A520 or VSVG3-SP-GFP proteins were homogeneously distributed on the NS-1 cell surface with strong polarization of GM1

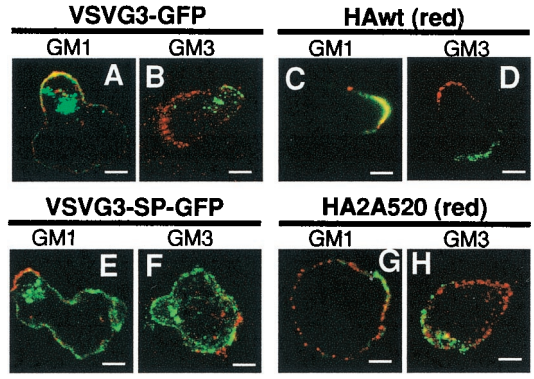

Fig. 4. Raft association is a requisite for membrane protein redistribution in polarized T cells. Distribution of VSVG3-GFP (*A* and *B*) or HA wild type (HAwt; *C* and *D*), and of mutants VSVG3-SP-GFP (*E* and *F*) or HA2A520 (*G* and *H*) in NS-1 cells was analyzed after copatching with anti-GM3 antibody or FITC-CTx, as indicated. The panels show red and green signal overlay. In the case of VSVG3 (green), GM1 and GM3 are visualized in red; for HAwt (red), GM1 and GM3 are in green. Colocalization is seen as yellow. The proportion of cells showing asymmetrical distribution was calculated by direct counting (n = 50–60) of transduced cells with a polarized phenotype. (Bar = 2 μm.)

(Fig. 4 *E* and *G*) and GM3 (Fig. 4 *F* and *H*). Quantitative analysis indicated that 85% of polarized, transduced NS-1 cells accumulated HA and VSVG3-GFP proteins preferentially at the uropod, whereas 14% of the NS-1 cells redistributed HA2A520 and VSVG3-SP-GFP proteins to a single cell pole. This result indicates that raft association is a major determinant for asymmetric protein redistribution in T cells.

Functional Role of Rafts in Polarization and Chemotaxis. To address the functional role of rafts in lymphocyte polarization, we studied the effect of cholesterol depletion on the acquisition of a migrating phenotype in NS-1 cells. Morphology and polarization marker redistribution were analyzed in cholesterol-depleted cells. CD treatment significantly reduces the number of NS-1 cells with a polarized phenotype, as well as the asymmetric redistribution of CD44 (Fig. 5 *A* and *B*). Cholesterol replenishment by incubating CD-treated cells with free cholesterol (20) restores the number of cells with a polarized phenotype (Fig. 5*B*), indicating that the CD inhibitory effect is limited to cholesterol removal.

Next, we studied whether cholesterol depletion affects specific uropod and leading-edge function. The ability to recruit bystander T cells was used as an indicator of uropod performance. As for polarization, CD treatment inhibits PBL recruitment to the Jurkat cell uropod, which was restored by replenishing cholesterol (Fig. 5*C*). The effect of cholesterol depletion on leading-edge function was tested by Jurkat cell chemotaxis toward SDF-1α, as CXCR4 localizes at this cell pole. CD treatment inhibited chemotaxis toward this chemokine, whereas cholesterol replenishment restored normal migration values (Fig. 5*D*). These data suggest a role for rafts in bystander T cell recruitment and lymphocyte chemotaxis, which require prior acquisition of a polarized phenotype.

Asymmetric U- and L-Raft Distribution Requires Intact Actin Cytoskeleton. Finally, we addressed the mechanism involved in raft redistribution by disrupting actin (latrunculin-B) or microtubule (demecolcine) cytoskeleton. Asymmetric distribution of GM1 and GM3 lipids was abolished in latrunculin-B-treated cells (Fig. 6*A*) but was preserved in demecolcine-treated cells (Fig. 6*B*). The actin cytoskeleton-associated receptor CD44 (1) is also homogeneously distributed in latrunculin-B-treated cells (Fig. 6*C*) but remains asymmetrical in demecolcine-treated cells (Fig. 6*D*). It is interesting to note that CD44 and GM1 colocalization is largely lost in latrunculin-treated cells, suggesting that raft partitioning of CD44

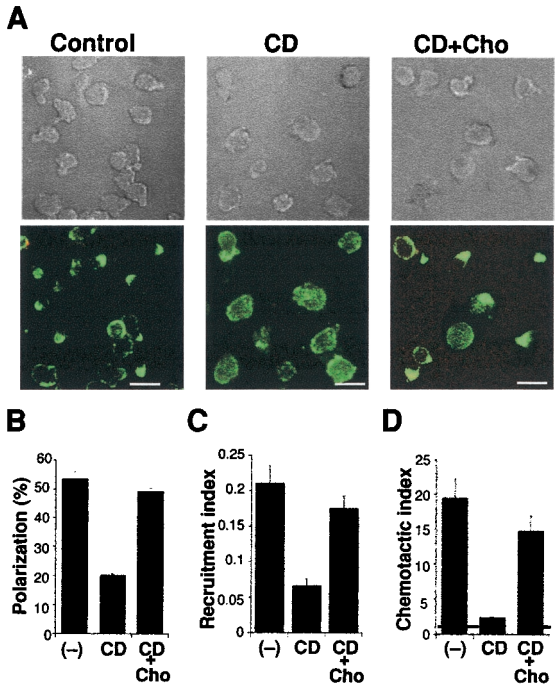

Fig. 5. Membrane rafts mediate the front–rear polarity required for T cell function. (*A*) Membrane cholesterol depletion impairs cell polarization. Panels show phase-contrast images (*Upper*) and CD44 distribution (*Lower*) of untreated (Control), CD-treated (CD), and cholesterol-replenished (CD+Cho) NS-1 cells. (Bar = 10 μm.) Bars in *B–D*: untreated (−), CD-treated (CD), and cholesterol replenished (CD+Cho). (*B*) Random fields (n = 8) in two independent experiments were recorded. Cells with a polarized phenotype (as determined by morphology and CD44-polarization) were counted directly. Total cells recorded: untreated, 250; CD-treated, 205; CD + Cho, 210. (*C*) Raft integrity is required for bystander T cell recruitment. Untreated, CD-treated, and cholesterol-replenished Jurkat cells were stimulated with SDF-1α and PBL recruitment was analyzed by direct counting. Data are expressed as a recruitment index (see *Materials and Methods*). (*D*) Cholesterol depletion inhibits cell chemotaxis. Untreated, CD-treated, and cholesterol-replenished Jurkat cells were assayed for chemotaxis toward SDF-1α. Cells in the lower chamber were recovered, and the number was estimated by flow cytometry. The figure shows the chemotactic index, calculated as described in *Materials and Methods*.

is regulated by the actin cytoskeleton. Collectively, these results show that asymmetric distribution of both L- and U-rafts specifically require actin cytoskeleton integrity.

Discussion

In migrating, a cell must integrate spatial and temporal information provided by environmental cues to correctly redistribute membrane receptors, adhesion proteins, and signaling molecules and to induce the cytoskeletal changes that lead to the polarized phenotype. Nonetheless, the mechanisms that effect this polarization are not fully understood. Asymmetry in constitutively polarized cells such as epithelia and neurons is achieved in part by sorting cargo proteins to specific membrane locations by using two post-Golgi circuits, one independent of and one dependent on protein clustering with lipid rafts (21). We have shown that protein clustering in raft domains also is needed for their redistribution to the leading edge of migrating adenocarcinoma cells (4), suggesting that initial segregation between raft and nonraft proteins in the trans-Golgi network may have a role in inducing a migrating phenotype in initially nonpolarized cells. Golgi integrity is required to generate and maintain cell asymmetry and directed cell migration (11, 22).

Three major lines of evidence indicate that partitioning in raft domains is pivotal in membrane protein distribution to specific locations during lymphocyte polarization. First, raft-associated proteins and lipids are asymmetrically distributed in T cells with a migrating phenotype. Second, proteins with no functional significance in cell polarization or migration segregate asymmetrically in migrating lymphocytes as a function of their raft association, and in addition, nonraft partitioned mutants are distributed homogeneously in polarized cells. Third, membrane cholesterol depletion impedes cell polarization and inhibits chemokine-induced chemotaxis.

These results concur with and amplify the concept of membrane rafts as necessary platforms for membrane receptor redistribution and acquisition of a polarized phenotype during carcinoma cell migration (4). Whereas GM1-enriched rafts accumulated at the leading pseudopodia in tumor cells, we observed segregation of two distinct types of raft domains that distribute to opposite edges in T cells—the GM3-enriched leading edge (L-raft) and the GM1-enriched uropod (U-raft). This difference between carcinoma cells and T cells may reflect distinct migration strategies (23). In carcinoma cells (as in fibroblasts), the leading edge consists of one or several pseudopodia that attach to the substrate; integrins and other adhesion receptors such as CD44 cluster prominently at the leading pseudopod where F-actin also accumulates. Moreover, blockage of cell-adhesion receptors with anti-integrin antibodies inhibits cell polarization and migration, indicating that integrin-mediated cytoskeletal linkages are needed to trigger migration in these cells (24, 25). In contrast, the leading edge of migrating T cells is weakly stained or negative for integrins and other adhesion receptors such as CD44 and ICAM-1 and -3, which concentrate at the uropod. Concurrently, focal adhesion kinase is phosphorylated and redistributed to the leading edge (26), whereas F-actin stains the uropod (27). This unique compartmentalization characterizes T cells as bipolar sensors optimized for cell–cell (at the U-raft) and cell–

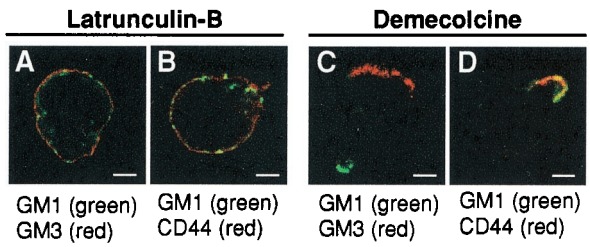

Fig. 6. Raft distribution requires intact actin cytoskeleton. NS-1 cells were treated with latrunculin-B (*A* and *B*) or demecolcine (*C* and *D*) and the distribution of GM1 and GM3 (*A* and *C*) or GM1 and CD44 (*B* and *D*) was analyzed by confocal microscopy. Images are representative of cells recorded (n = 40) in two independent experiments. (Bar = 2 μm.)

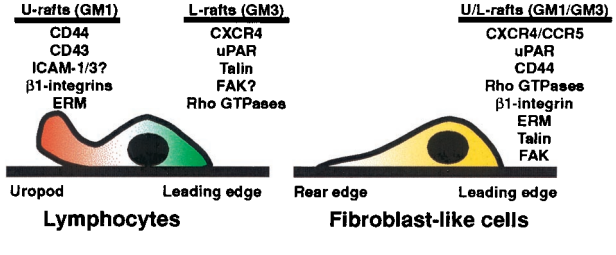

Fig. 7. Model for the redistribution of membrane rafts and associated proteins in migrating T cells and fibroblast-like cells. The scheme shows the segregation of U-rafts (GM1-enriched) and L-rafts (GM3-enriched) in migrating T cells, as well as the predictive association of membrane receptors and signaling molecules to each raft type, based on our results or those in literature (1, 36). In fibroblast-like cells, both U- and L-rafts probably redistribute to the leading edge; see *Discussion* for details. ERM, ezrin–radixin–moesin.

matrix (at the L-raft) interactions (28). Thus, the T cell uropod morphologically and functionally resembles the leading pseudopodia of fibroblast-like cells including GM1-enriched raft accumulation at this cell pole. Accordingly, ezrin–radixin–moesin proteins that link F-actin to the cytoplasmic tails of adhesion molecules partition in GM1-enriched rafts (29) and redistribute to the leading edge in fibroblasts (30) but redistribute to the uropod in lymphocytes (31).

There is also correspondence between leading-edge-redistributed molecules in fibroblast-like cells and T cells. Raft-associated proteins such as chemokine receptors and uPAR redistribute to the leading edge in migrating fibroblast-like cells (4, 32) and lymphocytes (1, 33). Different raft platforms are used—GM1 rafts in fibroblast-like cells and GM3 rafts in T cells. Two distinguishable GM3- and GM1-enriched raft subfractions also are reported in nonlymphoid cells (34, 35): the GM3 rafts are enriched in specific proteins such as FAK, Src family kinases, and the small Rho GTPases (36), all of which concentrate at the leading edge of migrating T cells (1). GM1- and GM3-enriched rafts may redistribute to the same cell pole in fibroblast-like cells (37). Known L- and U-raft markers are outlined in Fig. 7.

Asymmetric protein redistribution during polarization depends on raft association rather than on their functional significance in cell motility or signaling. A prominent role is reported for cytoskeletal interactions in CD43, CD44, and ICAM-3 redistribution to the uropod (1). VSVG3-GFP and HA are unlikely to associate with cytoskeleton or interact with other T cell membrane proteins; thus, their asymmetric redistribution may be caused by the coalescence of laterally diffusing rafts in specific cell locations such as the uropod. These results suggest that membrane receptor partitioning to rafts may occur upstream of their linkage to cytoskeleton and function as a mechanism for uropod redistribution. Nonetheless, an intact actin (but not tubulin) cytoskeleton is needed for L- and U-raft redistribution, concurring with other reports (38). Because ezrin–radixin–moesin proteins partition to rafts, raft association of CD43, CD44, and other adhesion receptors may favor their linkage to the cytoskeleton for correct redistribution.

The physiological implications of raft coalescence for acquisition of front–rear polarity and cell chemotaxis are evident, as it may provide a mechanism for the integration of distinct signaling pathways. That chemoattractant receptors partition in these domains suggests that asymmetrical raft redistribution amplifies chemotactic signal detection. The amplification may occur at the receptor level or downstream through local activation of chemotactic intermediates such as Rho GTPases and generation of phosphatidylinositol 4,5-bisphosphate, found in raft domains and at the leading edge of neutrophils (39). There is functional evidence that raft clustering may activate local signal transduction; indeed, compartmentalization of cell receptors and signaling molecules between raft and nonraft membrane domains is required for efficient antigen-mediated T cell activation (40).

In addition to the essential role of rafts as organizational principles in T cell receptor signaling and immunological synapse stabilization, we show that membrane rafts may also be a mechanism for local activation of signaling pathways involved in the cell asymmetries required for T cell migration.

We thank Drs. P. Labrador and J. Stein for critical reading of the manuscript, Drs. P. Keller and P. Scheiffele for gifts of VSVG and HA constructs, respectively, and for valuable discussion, and C. Mark for editorial assistance. This work was supported by grants from the Spanish Secretaría de Estado de Política Científica y Tecnológica/European Union, the Comunidad Autónoma de Madrid, and the Pharmacia Corporation. The Department of Immunology and Oncology was founded and is supported by the Spanish National Research Council and the Pharmacia Corporation.

1. Sánchez-Madrid, F. & del Pozo, M. (1999) *EMBO J.* **18,** 501–511.
2. Mañes, S., Mira, E., Gómez-Moutón, C., Lacalle, R. & Martínez-A., C. (2000) *IUBMB Life* **49,** 89–96.
3. Seveau, S., Keller, H., Maxfield, F., Piller, F. & Halbwachs-Mecarelli, L. (2000) *Blood* **95,** 2462–2470.
4. Mañes, S., Mira, E., Gómez-Moutón, C., Lacalle, R., Keller, P., Labrador, J. & Martinez-A., C. (1999) *EMBO J.* **18,** 6211–6220.
5. Harder, T. & Simons, K. (1999) *Eur. J. Immunol.* **29,** 556–562.
6. Moran, M. & Miceli, M. (1998) *Immunity* **9,** 787–796.
7. Rozelle, A., Machesky, L., Yamamoto, M., Driessens, M., Insall, R., Roth, M., Luby-Phelps, K., Marriott, G., Hall, A. & Yin, H. (2000) *Curr. Biol.* **10,** 311–320.
8. Scheiffele, P., Roth, M. & Simons, K. (1997) *EMBO J.* **16,** 5501–5508.
9. Toomre, D., Keller, P., White, J., Olivo, J. C. & Simons, K. (1999) *J. Cell Sci.* **112,** 21–33.
10. Keller, P., Toomre, D., Díaz, E., White, J. & Simons, K. (2001) *Nat. Cell Biol.* **3,** 140–149.
11. Mira, E., Lacalle, R., González, M., Gómez-Moutón, C., Abad, J., Bernad, A., Martínez-A., C. & Mañes, S. (2001) *EMBO Rep.* **2,** 151–156.
12. Campanero, M., Sánchez-Mateos, P., del Pozo, M. & Sánchez-Madrid, F. (1994) *J. Cell Biol.* **127,** 867–878.
13. Pelletier, A., van der Laan, L., Hildbrand, P., Siani, M., Thompson, D., Dawson, P., Torbett, B. & Salomon, D. (2000) *Blood* **96,** 2682–2690.
14. Hug, P., Lin, H., Korte, T., Xiao, X., Dimitrov, D., Wang, J., Puri, A. & Blumenthal, R. (2000) *J. Virol.* **74,** 6377–6385.
15. Mellado, M., Rodríguez-Frade, J. M., Mañes, S. & Martínez-A., C. (2001) *Annu. Rev. Immunol.* **19,** 397–421.
16. Kniep, B., Cinek, T., Angelisova, P. & Horejsi, V. (1994) *Biochem. Biophys. Res. Commun.* **203,** 1069–1075.
17. van der Goot, F. G. & Harder, T. (2001) *Semin. Immunol.* **13,** 89–97.
18. Röper, K., Corbeil, D. & Huttner, W. (2000) *Nat. Cell Biol.* **2,** 582–592.
19. Harder, T., Scheiffele, P., Verkade, P. & Simons, K. (1998) *J. Cell Biol.* **141,** 929–942.
20. Simons, M., Keller, P., De Strooper, B., Beyreuther, K., Dotti, C. & Simons, K. (1998) *Proc. Natl. Acad. Sci. USA* **95,** 6460–6464.
21. Simons, K. & Toomre, D. (2000) *Nat. Rev. Mol. Cell Biol.* **1,** 31–39.
22. Bershadsky, A. & Futerman, A. (1994) *Proc. Natl. Acad. Sci. USA* **91,** 5686–5689.
23. Friedl, P., Brocker, E. & Zanker, K. (1998) *Cell Adhes. Commun.* **6,** 225–236.
24. Huttenlocher, A., Ginsberg, M. & Horwitz, A. (1996) *J. Cell Biol.* **134,** 1551–1562.
25. Maaser, K., Wolf, K., Klein, C., Niggemann, B., Zänker, K., Brocker, E. & Friedl, P. (1999) *Mol. Biol. Cell* **10,** 3067–3079.
26. Entschladen, F., Niggemann, B., Zanker, K. & Friedl, P. (1997) *J. Immunol.* **159,** 3203–3210.
27. Sullivan, J. & Mandell, G. (1983) *Cell Motil.* **3,** 31–46.
28. Serrador, J., Nieto, M. & Sánchez-Madrid, F. (1999) *Trends Cell Biol.* **9,** 228–232.
29. Michaely, P., Mineo, C., Ying, Y. & Anderson, R. (1999) *J. Biol. Chem.* **274,** 21430–21436.
30. Amieva, M. & Furthmayr, H. (1995) *Exp. Cell Res.* **219,** 180–196.
31. Serrador, J., Alonso-Lebrero, J., del Pozo, M., Furthmayr, H., Schwartz-Albiez, R., Calvo, J., Lozano, F. & Sánchez-Madrid, F. (1997) *J. Cell Biol.* **138,** 1409–1423.
32. Mañes, S., del Real, G., Lacalle, R., Lucas, P., Gómez-Moutón, C., Sánchez-Palomino, S., Delgado, R., Alcamí, J., Mira, E. & Martínez-A., C. (2000) *EMBO Rep*. **1,** 190–196.
33. Estreicher, A., Muhlhauser, J., Carpentier, J., Orci, L. & Vassalli, J. (1990) *J. Cell Biol.* **111,** 783–792.
34. Iwabuchi, K., Handa, K. & Hakomori, S. (1998) *J. Biol. Chem.* **273,** 33766–33773.
35. Chigorno, V., Palestini, P., Sciannamblo, M., Dolo, V., Pavan, A., Tettamanti, G. & Sonnino, S. (2000) *Eur. J. Biochem.* **267,** 4187–4197.
36. Yamamura, S., Handa, K. & Hakomori, S. (1997) *Biochem. Biophys. Res. Commun.* **236,** 218–222.
37. Mañes, S., Lacalle, R., Gómez-Moutón, C., del Real, G., Mira, E. & Martínez-A., C. (2001) *Semin. Immunol.* **13,** 143–157.
38. Foger, N., Marhaba, R. & Zoller, M. (2001) *J. Cell Sci.* **114,** 1169–1178.
39. Servant, G., Weiner, O. D., Herzmark, P., Balla, T., Sedat, J. W. & Bourne, H. R. (2000) *Science* **287,** 1037–1040.
40. Janes, P., Ley, S., Magee, A. & Kabouridis, P. (2000) *Semin. Immunol.* **12,** 23–34.